



# Perfluoroalkyl substances in a firefighting training ground (FTG), distribution and potential future release



Christine Baduel\*, Christopher J. Paxman, Jochen F. Mueller

The University of Queensland, National Research Centre for Environmental Toxicology, (Entox), Coopers Plains, Brisbane, Queensland, Australia

## HIGHLIGHTS

- PFASs concentrations have been quantified at a FTG (up to 230  $\mu\text{g g}^{-1}$  for PFOS).
- PFAS have been found within the concrete up to 12 cm depth.
- The total mass load of 15 PFASs is estimated at 1.7 kg for the whole FTG.
- A transport model for PFOS, PFOA and 6:2FTS is created under field condition.
- FTG will keep emitting these chemicals in rainfall runoff for several years/decades.

## ARTICLE INFO

### Article history:

Received 31 July 2014

Received in revised form 3 February 2015

Accepted 4 March 2015

Available online 21 March 2015

### Keywords:

Perfluorinated chemicals

Firefighting training ground

Transport model

Leaching

AFFF

Contaminated infrastructure

## ABSTRACT

The present study investigates the occurrence and fate of 15 perfluoroalkyl substances (PFASs) and one fluorotelomer sulfonate from a firefighting training ground (FTG) that was contaminated by intensive use of aqueous film forming foams (AFFF). The contamination levels and their spatial and vertical distribution are assessed in the structure. At the surface of the pad, perfluorooctane sulphonate (PFOS) is the dominant PFASs measured, with concentration varying from 10 to 200  $\mu\text{g g}^{-1}$ . PFASs were also detected in a concrete core at up to 12 cm depth, suggesting the vertical movement and higher transport potential of shorter chain compounds. The estimated mass load of linear PFOS in this specific pad was >300 g with a total of 1.7 kg for the sum of all PFASs analyzed. The kinetics of desorption of PFOS, PFOA and 6:2FTS from the concrete into an overlying static water volume has been measured under field conditions at two constant temperatures. Fitting the desorption data and estimated rainfall/runoff to a kinetic model suggests that this and similar firefighting training pads will likely remain a source of PFASs for many decades ( $t_{0.5} = 25$  years for PFOS).

© 2015 Elsevier B.V. All rights reserved.

## 1. Introduction

Perfluoroalkyl substances (PFASs) have been the focus of many studies due to their widespread distribution in the environment, their toxicity and bio accumulative potential [1–3]. PFASs have been used in a wide variety of products including firefighting foams [4]. Aqueous film forming foams (AFFF) were developed in the early 1960s and manufactured by 3M, Ansul and National Foam Companies [5] for efficiently extinguishing hydrocarbon-fuel fires (i.e. gasoline and kerosene). Perfluoroalkyl substances are key components in this formulation because they lower the surface tension at the air-foam interface and form a film over the hydrocarbon fuel to prevent re-ignition [6–8]. The concentration and composition of PFASs in AFFF vary by year of production, fabrication

process and by manufacturer [6,9]. AFFF have been widely used at sites such as airports, oil refineries and military bases for emergency and training purposes [6]. Training exercises may occur on a weekly basis or even several times per week depending on the site. At firefighting training grounds, training pads normally consist of a bounded concrete slab on which stands a large mock-up unit (LMU). Hydrocarbon-fuel (e.g., kerosene) is discharged on the pad, or sprayed from fixtures attached to the LMU via high pressure lines, and ignited. Firefighters are then employed to extinguish the fire using either water only or firefighting foam and/or dry chemical powder (DCP). The resultant exposure has led to the training ground infrastructure being contaminated by perfluoroalkyl carboxylates (PFCAs), perfluoroalkyl sulfonates (PFASs), and fluorotelomer sulfonates (FTSs). Although the use of AFFF was discontinued in 2010 at the training facility; PFOS concentration levels of approximately 70–120  $\mu\text{g L}^{-1}$  were recorded in rainfall runoff from the pad in 2014. In other words, after being a sink of PFASs through several decades

\* Corresponding author. Tel.: +61 466390712.

E-mail address: [chris.baduel@hotmail.com](mailto:chris.baduel@hotmail.com) (C. Baduel).

of AFFF exposure, the concrete training pad was believed to become a source of these chemicals through water runoff.

The disposal of wastewater contaminated by AFFF components can be problematic, for the operators of training facilities and environmental regulators alike. Disposal options for contaminated water runoff include discharge to an on-site wastewater treatment (WWT) facility or sewer. The discharge of AFFF directly into the environment may lead to release of PFASs to groundwater and surface water at  $\mu\text{g L}^{-1}$  to  $\text{mg L}^{-1}$  levels [10–13]. Moreover, PFASs are not efficiently eliminated through the WWT process, hence the release into downstream water bodies and whole water catchment areas can occur [14]. PFASs in the aquatic environment can directly contribute to human exposures via drinking water [15] and aquatic products [11,16–20]. The U.S. Environmental Protection Agency recently implemented provisional health advisories for perfluorooctanoate (PFOA) and perfluorooctane sulfonate (PFOS) in drinking water, advising that levels should remain below 0.4 and  $0.2 \mu\text{g L}^{-1}$ , respectively.

Because PFASs are released in water runoff from fire training infrastructure, it is important to understand and estimate the factors controlling the transport of PFASs from the concrete training pad to the environment. Knowledge of the desorption mechanism of PFASs from concrete is particularly important for understanding the fate and transport mechanisms of PFASs via the water runoff from the firefighting ground facility.

This study assesses the distribution and fate of selected perfluoroalkyl carboxylates (PFCAs), perfluorinated sulfonic acids (PFASs), and a fluorotelomer sulfonate (FTS) at a fire training facility. The contamination profile of a firefighting ground infrastructure is first investigated by determining the surface and vertical mass load of 15 PFASs including 11 PFCAs (C4–C14 PFCAs) and 4 PFASs, (C4, C6, C8, C10 PFASs), and 1 fluorotelomer sulfonate (FTS, 6:2). The potential for surface transport of specific PFASs is then investigated by studying kinetic desorption of PFOS, PFOA and 6:2FTS under real conditions on a contaminated FTG. These results are used to constrain a kinetic model that is used to estimate the future concentration and emission of PFASs from a firefighting pad and assess the extent to which such pads are likely to remain a source of PFASs to the surrounding environments.

## 2. Materials and methods

### 2.1. Site characteristics

The site is located in Australia and has been an operational fire training facility since 1983. Until 2010, approximately 3000 L of AFFF concentrate were used every year in weekly training exercises at the site. The transition to fluorine free foam (Solberg®) occurred in 2010 and the remaining Ansulite stocks at each station were quarantined from use, pending their destruction. The station received new trucks which had never used Ansulite or other AFFF, so there would not have been any legacy contamination of PFASs from the trucks themselves. The site comprises a large steel mock-up unit (LMU) standing above a bounded concrete area (training pad). The size of the training pad is 19.7 m by 25.8 m and approximately 18 cm thick, representing an area of  $508 \text{ m}^2$  and a volume of approximately  $90 \text{ m}^3$  of concrete. Concrete is a heterogeneous material with a typical density of  $2400 \text{ kg m}^{-3}$  [21], produced by mixing coarse aggregates such as sand and pebbles with water and cement. Through a chemical reaction called hydration; the cement paste hardens and gains strength. In the following, we estimate the PFASs mass load within the concrete without attempting to differentiate between each individual component of the concrete. While a measurement of a small amount of concrete sample might be affected by heterogeneities (e.g., presence of pebbles), sufficient sampled material ( $\approx 2\text{--}3 \text{ g}$ ) was collected at each sample point per site to ensure adequate representation of the heterogeneous material. Although we know that AFFF was applied only between 1983 and 2010, we cannot estimate the quantity of PFASs that was used and the quantity that was actually adsorbed onto the concrete infrastructure over that period. Therefore, we need to rely on present-day measurements in this study. The FTG assessed is considered to be typical of many firefighting grounds within Australia that have been or are currently being exposed to AFFFs.

### 2.2. Concrete sample collection

Concrete samples collection was carried out on the same day while the training pad was completely dry. To determine the mass

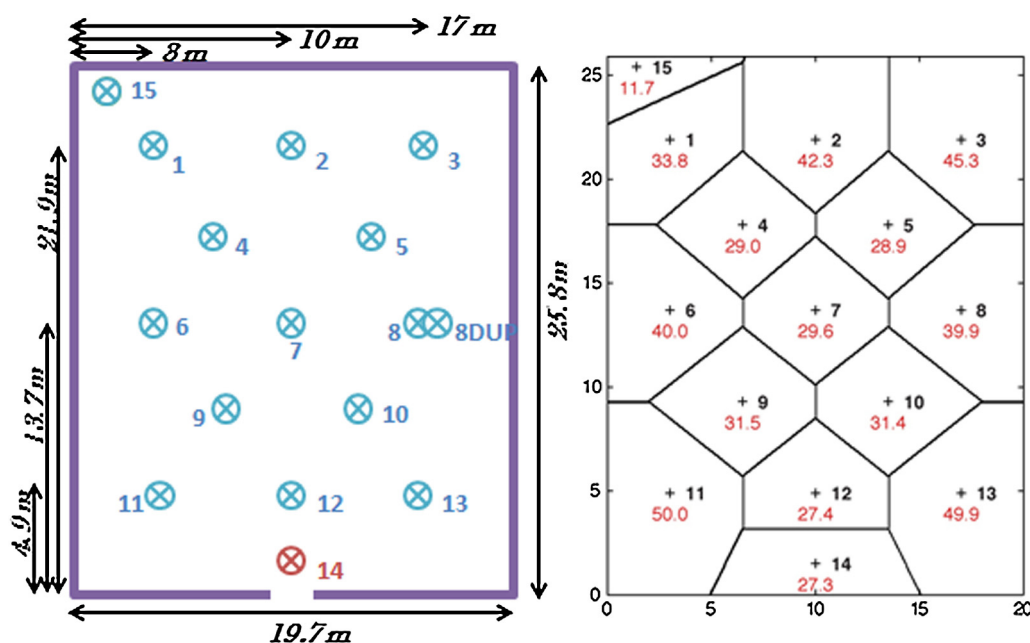


Fig. 1. (a) Sample collection sites and size of the training pad. Site 14 (in red) is where the depth profile occurred. (b) Each sample is representative of the area ( $\text{m}^2$ ) written in red in the figure. (For interpretation of the references to color in this figure legend, the reader is referred to the web version of this article.)

load and the spatial distribution of PFASs throughout the pad, concrete powder was collected at the surface of the pad down to 5 mm deep using a drill ( $\varnothing=4$  mm). The powder was collected using a metallic spatula and stored in a ziplock bag until analysis. Approximately 10 holes were drilled at each site to collect 2–3 g of concrete powder. The extracted powder was then pooled and homogenized to constitute a sample. At site #8 a duplicate was collected to investigate variability of the sampling technique (Supplementary material S2). Concrete samples were collected at 15 locations on the pad numbered from #1 to #15 as shown in Fig. 1a. Each sampling site from #1 to #14 is representative of an area varying from 27 to 50 m<sup>2</sup> (Fig. 1b). To accurately measure the penetration depth of PFASs within the concrete pad, a large core (10 cm × 13 cm × 14 cm) was removed from the pad (at site #14) using a power cutting disk. The core was then stored at  $-20^{\circ}\text{C}$ . To estimate the vertical profile of the concrete core, concrete powder was collected by drilling on the side of the core every centimeter down to 12 cm. Approximately 2 g of cement were collected at each depth and pooled. Only 0.1 g of cement powder was used for the extraction and quantification of PFASs. Between two successive drillings, the side of the core was brushed to remove any residual dust and to limit cross contamination of the subsequent samples. The brushing off of the residual dust was sufficient to avoid major cross contamination as evidenced by the good reproducibility of the duplicate and the wide range of measured concentrations of the two vertical profiles presented in the table S3 (Supplementary material).

Supplementary material related to this article found, in the online version, at <http://dx.doi.org/10.1016/j.jhazmat.2015.03.007>.

### 2.3. Kinetic desorption experiments

AFFF formulations are complex and include hydrocarbon surfactants, solvents, inorganic salts and corrosion inhibitors. Transport

of PFASs at the FTG may thus be influenced by other AFFF components and co-contaminants released during training exercises such as fuel [22]. Therefore, the kinetics of PFASs desorption was directly measured on the surface of the concrete core extracted from the pad. To maintain the water on the concrete surface, a plastic frame (ID 90 mm) was sealed onto the surface ( $\approx 64$  cm<sup>2</sup>) of the concrete using a silicon adhesive/sealant (Selley's®). The frame was filled with 100 mL of MilliQ water, which is equivalent to a depth of 15 mm in the frame and corresponds to the amount of water brought by a strong rain event (rainwater) or consecutive training exercises (using tap water) at the pad location. MilliQ water was selected as a surrogate for both rainwater and tap water to facilitate the experiment. The  $\text{pK}_a$  values of PFOS and PFOA reported were around 3.27 and 2.8, respectively [23,24], both lower than the pH values 6 or 8. Therefore, PFOS and PFOA mainly existed in deprotonated forms within the pH range of 6 (pH of MilliQ water) or 8 (pH of rainwater). So no difference should be observed for this pH range. The use of a volume of 100 mL ensures a quasi-unchanged volume when 0.49 mL was drawn for analysis at various time intervals. This volume of water was collected at different time intervals and spiked with <sup>13</sup>C-labelled solution mixture (2 ng) and performance standards <sup>13</sup>C<sub>8</sub>-PFOS (2 ng) and <sup>13</sup>C<sub>8</sub>-PFOA (2 ng) prior analysis. To avoid evaporation during the kinetic desorption experiment, parafilm® was used to cover the plastic frame. As concrete is a porous media, to determine any significant water loss by absorption by the concrete or by evaporation, the volume of water collected at the end of the experiment was measured. The kinetic experiments were undertaken two times consecutively on the surface of the concrete core and at two constant and controlled temperatures of 4 °C and 24 °C. These temperatures are representative of lower and upper range air temperature at FTG location. The desorption experiments have been undertaken sequentially. As both led to similar curves they have been joined together to calculate the fit

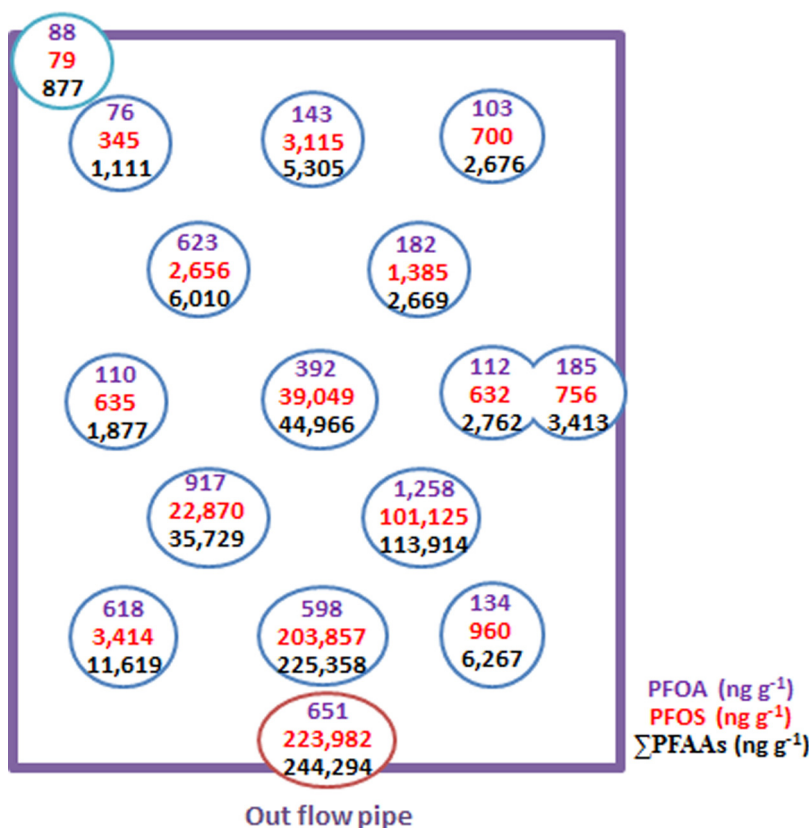


Fig. 2. Concentration (ng g<sup>-1</sup>) of PFOA, PFOS and  $\Sigma$ PFASs at 15 sites over the training pad.

parameters. Indeed the sequential approach is valid given that the concentration in the concrete remained largely unchanged after the first desorption experiment.

#### 2.4. Materials

The PFACs investigated in this work were perfluorobutanoic (PFBA), perfluoropentanoate (PFPA), perfluorohexanoate (PFHxA), perfluoroheptanoate (PFHpA), perfluorooctanoate (PFOA), perfluorononanoate (PFNA), perfluorodecanoate (PFDA), perfluoroundecanoate (PFUnA), perfluorododecanoate (PFDoA), perfluorotridecanoate (PFTriA), and perfluorotetradecanoate (PFTeA). The PFASs were perfluorobutane sulfonate (PFBS), perfluorohexane sulfonate (PFHxS), perfluorooctane sulfonate (PFOS) and perfluorodecane sulfonate (PFDS). The native PFACs and PFASs solution mixture (MixB) were purchased from Wellington Laboratories, Guelph, Ontario, Canada. The  $^{13}\text{C}$ -labelled PFAC and PFAS solution mixture (MPFAC-MXA) was obtained from Wellington Laboratories, Guelph, Ontario, Canada and contained: perfluoro[1,2,3,4- $^{13}\text{C}_4$ ]butanoic acid, perfluoro[1,2- $^{13}\text{C}_2$ ]hexanoic acid, perfluoro[1,2,3,4- $^{13}\text{C}_4$ ]octanoic acid, perfluoro[1,2,3,4,5- $^{13}\text{C}_5$ ]nonanoic acid, perfluoro[1,2- $^{13}\text{C}_2$ ]decanoic acid, perfluoro[1,2- $^{13}\text{C}_2$ ]undecanoic acid, perfluoro[1,2- $^{13}\text{C}_2$ ]dodecanoic acid, sodium perfluoro-1-hexane[ $^{18}\text{O}_2$ ]sulfonate, sodium perfluoro-1-[1,2,3,4- $^{13}\text{C}_4$ ]octanesulfonate. A  $^{13}\text{C}$ -labelled instrument performance internal standard perfluoro[ $^{13}\text{C}_8$ ]octanoic acid ( $^{13}\text{C}_8$ -PFOA) and perfluoro[ $^{13}\text{C}_8$ ]octanesulfonate ( $^{13}\text{C}_8$ -PFOS) were purchased from Wellington Laboratories (Guelph, Ontario, Canada). High purity solvents were purchased from Merck (Darmstadt, Germany). Water was purified through a MilliQ system (Millipore, 0.22  $\mu\text{m}$  filtered, 18.2  $\text{m}\Omega\text{ cm}^{-1}$ ). Mobile phases were filtered using Phenex 0.20  $\mu\text{m}$  47 mm nylon filter membranes (Lane Cove, Australia).

#### 2.5. Concrete sample extraction

The concrete powder was placed in a polypropylene tube (falcon<sup>®</sup>) and extracted with 4 mL of methanol (Merck<sup>®</sup>) under sonication for 15 min. After sonication the samples were centrifuged (Beckman Coulter, Allegra X-15R) for 15 min at 2090 g-force and the supernatant transferred to another prewashed polypropylene tube. The concrete powder was extracted a second time using 2 mL of methanol for 15 min in an ultrasonic bath. After centrifugation the two extracts were combined. From this final volume only 200  $\mu\text{L}$

**Table 1**  
Concentration ( $\text{ng g}^{-1}$ ) for 15PFASs and 1 fluorotelomer sulfonate over the pad, presenting the minimum, maximum and spatial mean value.

Chemicals (linear form)	Concentration ( $\text{ng g}^{-1}$ )		
	Min	Max	Spatial mean
PFBA	–	659	158
PFPA	14	530	143
PFHxA	63	3,749	865
PFHpA	31	612	201
PFOA	76	1,259	414
PFNA	11	1,009	97
PFDeA	30	6,641	831
PFUnA	6	4,505	709
PFDoA	26	2,698	863
PFTriA	15	594	290
PFTeA	20	1,017	300
PFBS	11	2,177	514
PFHxS	115	4,391	1,173
PFOS	79	223,983	33,426
PFDS	10	473	80
6:2FTS	23	553	93
$\sum$ PFASs	877	244,294	40,157

(or 10  $\mu\text{L}$  for the more concentrated sample) was transferred to a propylene vial and filled up to 500  $\mu\text{L}$  with 5 mM of ammonium acetate and spiked with  $^{13}\text{C}$ -labelled solution mixture (2 ng). Finally the performance standards  $^{13}\text{C}_8$ -PFOS (2 ng) and  $^{13}\text{C}_8$ -PFOA (2 ng) were added to the vial for volume corrections and to compensate for instrumental drift.

#### 2.6. Chemical analysis

The PFASs of interest in the concrete extracts and water samples were analyzed using high performance liquid chromatography (HPLC, Shimadzu Corp., Kyoto Japan) coupled to a tandem mass spectrometer (QTrap 5500AB-Sciex, Concord, Ontario, Ca). The injected volume was 5  $\mu\text{L}$ . The targeted PFASs were separated on a Gemini C18 column (50 mm  $\times$  2 mm i.d. 3  $\mu\text{m}$  110 Å) (Phenomenex, Torrance, CA) and through gradient elution using mobile phases made of 10% and 90% methanol, respectively, with 5 mM ammonium acetate. The mass spectrometer was operated in negative electrospray ionisation mode using scheduled multiple reaction monitoring (SMRM) [28,29]. An extra guard column ( $\text{C}_{18}$ ) was installed between the solvent reservoirs and the injector to exclude PFASs that originated from the HPLC system. Identification and confirmation were achieved using retention time and comparing ratio of SMRM transition intensity between the samples and the standards in the same batch of analysis. Quantification was achieved using  $^{13}\text{C}$ -labelled chemicals of PFACs and PFASs. Calibration standards were made up in 500  $\mu\text{L}$  (300  $\mu\text{L}$  methanol/200  $\mu\text{L}$  using 5 mM ammonium acetate in water in the range between 0.1 and 100  $\text{ng mL}^{-1}$  (0.1; 0.2; 1; 4; 10; 20; 40; 100). Only the linear isomer of individual PFASs has been quantified, even if isomers were detected in all the samples.

#### 2.7. Quality assurance

Calibration standards were injected three times in each batch of samples. Quality control standards were added to the batch and injected after every 10 samples to check for instrument drift. Quantification of PFASs was performed using a linear regression fit analysis weighted by  $1/x$  of the calibration curve. The quantitation of PFASs was based upon comparison with calibration curves constructed using only the linear isomer of each compound. Instrumental detection limits (DL) were set according to three times the standard deviation of the concentration of the lowest standard after eight injections of this standard. Limits of quantitation (LOQ) were set at nine times the standard deviation. LOQs were analyte and matrix dependent but were approximately 1–13  $\text{ng g}^{-1}$  in concrete extract and 0.05–0.20  $\text{ng L}^{-1}$  in aqueous samples. All values reported are corrected for recovery of the surrogate standards which were greater than 60% for all samples in all matrices (S1, Supplementary material). Samples of procedural blank (MilliQ water for water samples, and unexposed to AFFF concrete), duplicates and matrix spikes were prepared in each batch of samples and treated in the same way as the real samples. Both procedural and instrumental blanks showed no PFASs contaminations.

Supplementary material related to this article found, in the online version, at <http://dx.doi.org/10.1016/j.jhazmat.2015.03.007>.

### 3. Results and discussion

#### 3.1. Spatial variation

All of the 16 investigated compounds have been detected in the surface layer of the pad. The concentrations of PFOS, PFOA and the sum of all PFASs are shown in Fig. 2. The spatial mean concentration of individual PFASs is estimated (Table 1) across the entire pad using the 15 sites concentrations weighted by the area corresponding to

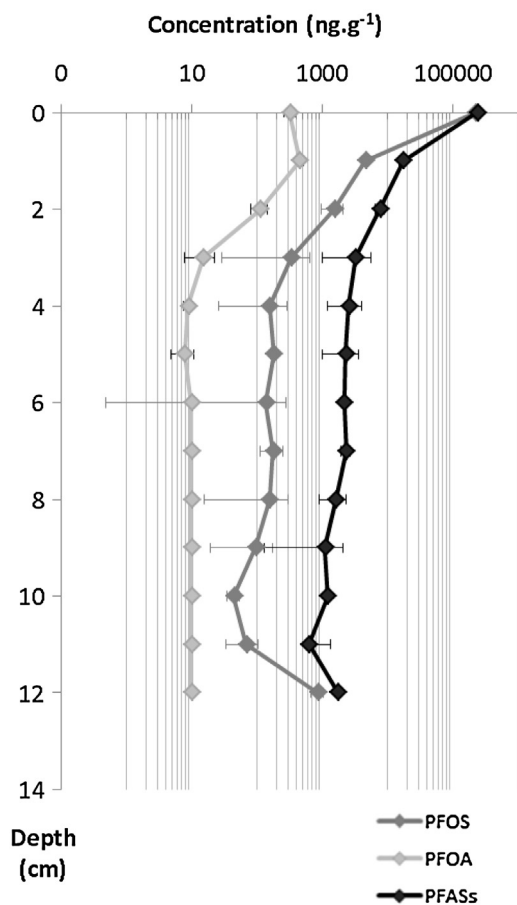


**Fig. 3.** Vertical profile contamination ( $\text{ng g}^{-1}$ ) of PFOS, PFOA and  $\Sigma$ PFASs in the concrete at site #14 close to the out flow pipe. The concentration is an average of the two core profiles and the error bars represent the standard variation between these two values. More compounds are presented in Supplementary material S3(b).

each sampling site, as presented in Fig. 1. All compounds (e.g., S2 Supplementary material) present a higher concentration near the center of the pad under the LMU, and close to the drainage pipe where water tends to pool after rain events and training exercises. In particular, the PFOS concentration greatly varies over the pad, from  $80 \text{ ng g}^{-1}$  at one extreme corner of the pad to  $200,000 \text{ ng g}^{-1}$  close to the drainage pipe. This demonstrates that there can be several orders of magnitude between concentrations at two locations on the pad. The highest surface mean concentrations have been found for PFOS ( $33 \mu\text{g g}^{-1}$ ), followed by PFHxS ( $1173 \text{ ng g}^{-1}$ ), PFHxA, and PFCAs with longer perfluoroalkyl chains such as PFDeA, PFUnA and PFDoA ( $700\text{--}900 \text{ ng g}^{-1}$ ).

### 3.2. Vertical distribution

Two vertical profiles were taken from the concrete core collected at the FTG (site #14) to determine the penetration of the chemicals through the material. Fig. 3 represents the average concentrations of PFOS, PFOA and  $\Sigma$ PFASs in the concrete at different depths between 0 and 12 cm. The PFOS and PFOA concentrations

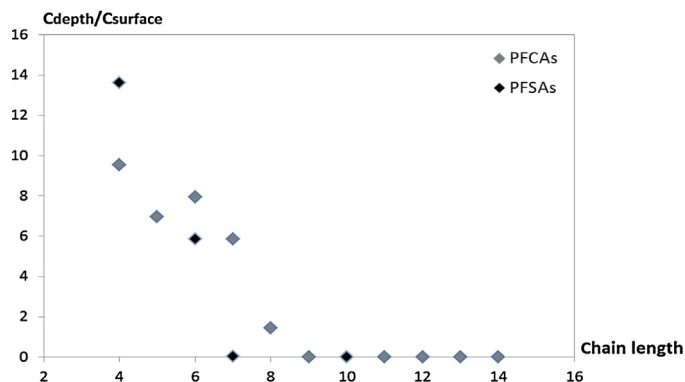


**Fig. 4.** Ratio of the concentration at 1 cm depth to the concentration at the surface of the core for individual PFASs (collected at site #14) versus the number of carbons in the perfluorinated carbon chain.

significantly decrease with depth, with the highest concentration measured at the surface of the pad. PFASs with perfluoroalkyl chain of less than 9 carbons are observed at all depths of the concrete (e.g. S3(a) and (b), Supplementary material). A downward vertical leaching behavior is clearly observed for the shorter chain PFASs (PFBA, PFPA, PFHxA and PFBS) which present a constant concentration through the entire core. PFCAs with a longer perfluorinated chain from 9 to 14 carbons are detected exclusively at the surface of the training pad. Fig. 4 shows that the penetration depth decreases with the number of carbons in the perfluorinated carbon chain (the carboxylate-contained carbon is not included). This observation suggests that the PFASs with a short perfluoroalkyl chain leach more efficiently through the concrete and may impact underlying groundwater. Similar observations have been observed in soil samples [22,25].

### 3.3. Total mass load in the training pad

The total mass load of individual PFASs within the first five millimeters and for the whole training pad has been estimated and is presented in Table 2. We assume that each concentration  $c_i$  measured at one of the 15 sites is representative of an area  $A_i$  as shown in Fig. 1b. As concentrations are all determined for the first 5 mm, the total mass load  $M_{\text{srf}}$  in the surface layer of the pad (0–5 mm) is given by:

$$M_{\text{srf}} = \sum_{i=1}^{15} c_{i0} a_i h \rho$$

where  $\rho$  is the density of the concrete,  $h = 5 \text{ mm}$  and  $c_{i0}$  is the mean concentration in the surface layer at site  $i$ .

Similarly, the total mass load  $M_{\text{tot}}$  would be defined as:

$$M_{\text{tot}} = \sum_{i=1}^{15} \sum_{k=1}^N c_{ik} a_i h_k \rho$$

where  $\rho$  is the density of the concrete,  $h_k$  is the thickness of layer  $k$  (with a total of  $N$  vertical layers), and  $c_{ik}$  the mean concentration at site  $i$  and layer  $k$ . Unfortunately, we could not extract cores all over the pad, so we have to make an assumption on the vertical distribution. Having in mind that PFASs within the concrete originally come from the surface, it seems reasonable to assume that

**Table 2**  
Mass of individual PFASs (g) at the surface of the pad (0–0.5 cm) and in the total pad (0–12 cm).

	PFCAs (g)				PFASs (g)								FTS (g)	Total (g)			
	PFBA	PFPA	PFHxA	PFHpA	PFOA	PFNA	PFDeA	PFUnA	PFDoA	PFTriA	PFTeA	PFBS			PFHxS	PFOS	PFDS
Mass at the surface (0–0.5 cm)	1	0.9	5.4	1.3	2.6	0.6	5.2	4.4	5.5	1.8	0.5	3.2	7.3	208	0.5	0.6	250
Mass total (0–12 cm)	92	75	293	3	16	1.2	9	7	9	3	4	586	155	346	1	65	1,693

**Table 3**

Kinetic parameters deduced for PFOS, PFOA and 6:2FTS and Cc values measured at the surface of the core. Cc is expressed in  $\text{ng g}^{-1}$  of concrete,  $c_{\text{eq}}$  in  $\text{ng mL}^{-1}$ , and  $K_{\text{eq}}$  in  $\text{mL g}^{-1}$  ( $=\text{Cc}/c_{\text{eq}}$ ).

	Cc	$c_{\text{eq}}$ (24 °C)	$c_{\text{eq}}$ (4 °C)	$K_{\text{eq}}$ (24 °C)	$K_{\text{eq}}$ (4 °C)	A	B
PFOA	323	3.63	1.40	88.8	229.9	0.000169	3912.6
PFOS	227,498	106.8	56.3	2130.1	4040.8	0.300079	2633.7
6:2FTS	22	0.382	0.135	56.3	159.3	0.000031	4278.6

the concentration within the pad at a given site is proportional to the concentration within the surface layer at the same location. Mathematically, this assumption is expressed as:

$$c_{ik} = \alpha_k c_{i0}$$

where  $\alpha_k$  is only a function of depth, and is calculated from measurements from the core at site 14.  $\alpha_k$  also depends on the physical properties of individual compounds. From this, we obtain:

$$M_{\text{tot}} \approx \sum_{i=1}^{15} \sum_{k=1}^N c_{i0} \alpha_k a_i h_k \rho$$

The total mass of PFASs in the surface layer of the pad (0–0.5 cm) is estimated as ~250 g and ~1700 g within the whole pad. The total mass of PFOS in the surface layer and in the whole pad (down to 12 cm depth) is estimated at 208 and 346 g, respectively. For the shorter chains ( $C < 6$ ) the mass at the surface of the pad is quite low in comparison to the mass in the whole structure. This suggests that either most of these chemicals in the surface layer have been removed through water runoff from rainfall and firefighting exercises, or that the chemicals that were originally adsorbed in the surface layer have moved into deeper layers.

#### 3.4. Kinetics and thermodynamics of desorption

The kinetics of desorption measured from the surface of the core are shown in Fig. 5 for three compounds at two different constant temperatures. When pure water is poured on the concrete, the concentration of chemicals in water increases at an exponentially decreasing rate ( $1 - e^{-kt}$ ) and reaches a steady state after some time. The value of the steady-state concentration is affected by temperature and is 2–3 times higher at 24 °C than at 4 °C for the three compounds. As shown in Table 3, the ratio of the steady state concentration in water ( $c_{\text{eq}}$ ) to the concentration in the concrete surface layer (Cc) is very small. The concentration in water is indeed 2–3 orders of magnitude smaller than in the concrete for PFOA and 6:2FTS, and 3–4 orders of magnitude smaller for PFOS. These results are consistent with the fact that PFASs are still found in the concrete infrastructure several years after being impacted because it means that each rainfall event or firefighting exercise will only desorb a very small quantity of PFASs from the pad.

As one of the objectives of this study was to evaluate future and on-going PFASs concentration releases from the concrete infrastructure, we were required to develop a model to estimate PFASs desorption into water runoff. From the kinetic and thermodynamic laws commonly used to study desorption processes (see S4, Supplementary material), we can express the concentration in water as:

$$C(x, y, T, t) = Cc(x, y, t) \times \left(\frac{1}{A}\right) \times e^{-B/T} \times (1 - e^{-kt}) \quad (1)$$

where  $C(x, y, T, t)$  is the concentration in water at location  $(x, y)$ , absolute temperature  $T$ , and time  $t$ . Cc is the concentration in the concrete surface layer,  $A$  and  $B$  are thermodynamic constants, and  $k$  is the kinetic rate constant. Note that Cc is time-dependent over long periods (typically several years) but does not vary significantly over a few days (i.e., it can be considered as constant during a single desorption event). The three constants  $A$ ,  $B$  and  $k$  can be obtained by fitting Eq. (1) to the observed kinetics shown in Fig. 5 combined

with measurements of Cc from the previous subsections (see S4, Supplementary material).

Supplementary material related to this article found, in the online version, at <http://dx.doi.org/10.1016/j.jhazmat.2015.03.007>.

#### 3.5. Estimates of the time frame for PFOA, PFOS and 6:2FTS desorption from the FTG

In the previous subsection, we have assumed that the quantity of PFASs in the concrete is constant, which is a valid approximation for short periods (typically a few days long). In this subsection, the aim is to describe the change in the quantity of PFASs in the concrete over longer periods (several years). The result is not straight forward because the flux of PFASs emitted by the concrete structure into the water runoff depends on PFASs concentrations in the pad (as indicated in the previous subsection). Therefore, a model was required to be developed and used to estimate the timescale needed by the pad to release 50% and 90% of its PFASs.

First, we need to calculate the amount of chemicals released by the pad during a rainfall event or a firefighting exercise. We make the calculation for the case where rainwater is retained for one day on the surface of the training pad before being released to the waste water treatment facility (which was a common practise at this site). As shown above the concentration in water is almost at steady state for any PFASs (see previous sub-section). Hence the spatial mean concentration in water over the pad  $\langle C \rangle$  can be expressed as:

$$\langle C \rangle = \langle Cc \rangle \times \left(\frac{1}{A}\right) \times e^{-B/T} \quad (2)$$

where  $\langle C \rangle$  is the concentration of chemicals represented at the surface (0–5 mm) of the entire training pad (in  $\text{ng g}^{-1}$ ), and  $A$  and  $B$  are the thermodynamic constants found in the previous subsection. Consequently, for a quantity of rain  $r$  received on a given day (in mm), the mass of compounds  $q$  released by the pad can be estimated as:

$$q = r \times S \times \langle Cc \rangle \times \left(\frac{1}{A}\right) \times e^{-B/T} \quad (3)$$

where  $S$  is the surface of the pad (in  $\text{m}^2$ ). Adding up all rainfall events and training exercises over one year, and assuming that does not significantly vary over the year, the total flux of chemical ( $Q$ ) released by the pad can be expressed as:

$$Q = R \times S \times \langle Cc \rangle \times \left(\frac{1}{A}\right) \times e^{-B/T} \quad (4)$$

where  $R$  is the total water runoff in one year (from rain and firefighting training). This implies that the variation of chemical concentration in the concrete  $d\langle Cc \rangle$  during a time period of  $dt$  years can be expressed as:

$$\rho \times S \times h \times d\langle Cc \rangle = -R \times S \times \langle Cc \rangle \times \left(\frac{1}{A}\right) \times e^{-B/T} \times dt \quad (5)$$

where  $\rho$  and  $h$  are the concrete density and thickness, respectively. Consistently with the previous subsection,  $\langle Cc \rangle$  is representative of the surface layer (0–5 mm), so  $h$  is taken as 5 mm. There are two approximations made in Eq. (5). The first is that concentrations in the surface layer evolve homogeneously over long periods of time, which implicitly means that diffusion of PFASs is effective within

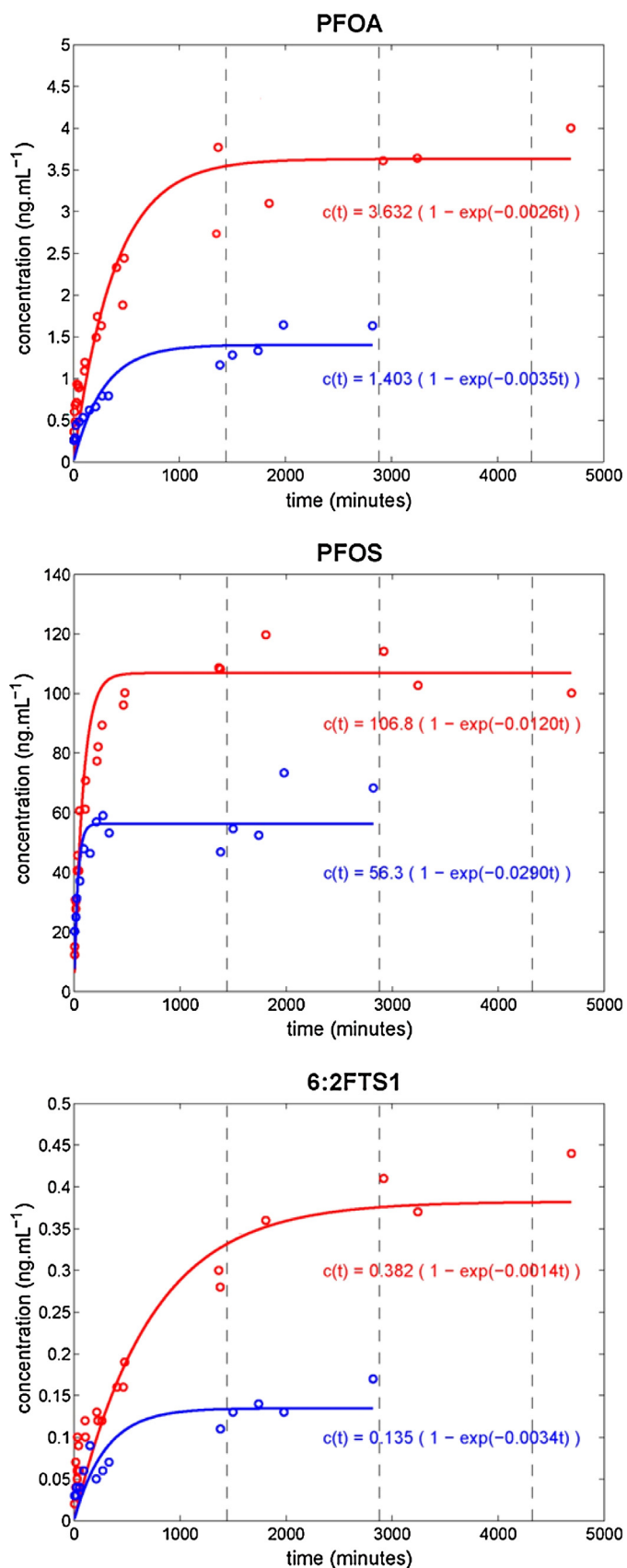


**Fig. 5.** Kinetics of desorption for PFOA (upper panel), PFOS (middle panel) and 6:2FTS (lower panel) at a constant temperature of 24 °C (red) and 4 °C (blue). Vertical dashed lines indicate every 24 h from the beginning of the experiment. The least-mean-square fit is represented using a solid line, and the corresponding equation is indicated below the line. (For interpretation of the references to color in this figure legend, the reader is referred to the web version of this article.)

the first 5 mm. The second approximation is that there is no upward flux of PFASs from underneath the surface layer. It is difficult to assess whether this is a strong assumption because we do not have measurements of PFAS diffusion or transport through concrete. Classical diffusion laws indicate a characteristic length of diffusion evolving as the square root of time, which would qualitatively justify a fast diffusion in the 5 mm surface layer and a much slower diffusion throughout the 18 cm. However, further work would be needed to define the surface layer thickness on physical bases.

Coming back to Eq. (5), it means that  $t$  the long-term desorption can be described by a first-order differential equation. Its solution is:

$$\langle Cc \rangle(t) = \langle Cc \rangle_{2014} \times e^{-t/\tau} \quad (6)$$

$$\text{with } \tau = \frac{A \times h \times \rho \times e^{B/T}}{R} \quad (7)$$

where  $\langle Cc \rangle_{2014}$  is the present concentration obtained in this study. The two last equations indicate a decrease of concentration in concrete at an exponentially decreasing rate from the pad. We now use this model to estimate the time needed for the training pad to release 50% and 90% of the present quantity of chemicals. From Eq. (6), we can see that this corresponds to times of 0.69  $\tau$  and 2.30  $\tau$ , respectively, so these times can be calculated from Eq. (7). Meteorological station data at the location of the pad indicate an average total annual rainfall  $R$  of approximately 500 mm. The weekly training represents an annual water addition of 208 mm. So it is estimated that a total amount of water of approximately 708 mm flow annually on the pad at this specific location. The mean concentration at the surface is estimated for the entire pad weighted by the area corresponding to each sampling site as presented in Fig. 1. Mean concentrations of PFOS, PFOA and 6:2FTS at the surface of the whole pad is estimated to be 33,425 ng g<sup>-1</sup>, 434 ng g<sup>-1</sup> and 100 ng g<sup>-1</sup>, respectively (Table 1). The result is that water runoff from rainfall and firefighting exercises should remove 50% of PFOS, PFOA and 6:2FTS in 25, 1 and 0.7 years, respectively. The time estimated to desorb 90% of these chemicals is 82, 4 and 2 years, respectively. The variation of the concentration of the PFOS in water runoff has been estimated over times as the concrete pad mass is depleted (combining Eqs. (2) and (6)). It is estimated that the PFOS concentration in water will reach 0.2  $\mu\text{g L}^{-1}$  in 2230 (0.2  $\mu\text{g L}^{-1}$  is the U.S.E.P.A health advisory threshold in drinking water) (S5, Supplementary material).

Supplementary material related to this article found, in the online version, at <http://dx.doi.org/10.1016/j.jhazmat.2015.03.007>.

#### 4. Conclusions

In this study we measured the spatial distribution and the vertical profile of 15 perfluoroalkyl substances and one fluorotelomer sulfonate at a fire fighting training facility. The total mass of PFASs found at the surface (0–0.5 cm deep) of the concrete pad is estimated at 250 g and 1700 g in the whole pad (0–12 cm deep). The estimated mass load of PFASs shows that the firefighting training pad contains significant PFASs and is likely to be an important source of long-term release. The training pad is projected to keep emitting PFOS and PFOA via rainfall runoff for several decades. The firefighting facility assessed is considered to be typical of many firefighting grounds extant in Australia that have or are currently being exposed to AFFFs. Understanding that this mass load estimation represents a scenario at one firefighting facility only, the results obtained from this study may be considered to be translatable to other concrete-lined industrial and domestic facilities that have been exposed to PFASs on a frequent basis.

## Acknowledgements

Dr. Jochen Mueller is funded through an ARC Future Fellowship (FF 120100546). The LC–MS/MS was funded through a Linkage Infrastructure, Equipment and Facilities (LIEF) Grant (LE 110100032). EnTox is a joint venture of The University of Queensland and Queensland Health and Forensic Scientific Services (QHFSS).

## References

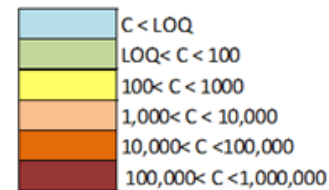
- [1] A.B. Lindstrom, M.J. Strynar, E.L. Libelo, Polyfluorinated compounds: past, present, and future, *Environ. Sci. Technol.* 45 (2011) 7954–7961.
- [2] R. Sturm, L. Ahrens, Trends of polyfluoroalkyl compounds in marine biota and in humans, *Environ. Chem.* 7 (2010) 457–484.
- [3] C. Lau, K. Anitole, C. Hodes, D. Lai, A. Pfahles-Hutchens, J. Seed, Perfluoroalkyl acids: a review of monitoring and toxicological findings, *Toxicol. Sci.* 99 (2007) 366–394.
- [4] M.M. Schultz, D.F. Barofsky, J.A. Field, Fluorinated alkyl surfactants, *Environ. Eng. Sci.* 20 (2003).
- [5] B.J. Place, J.A. Field, Identification of novel fluorochemicals in aqueous film-forming foams used by the US Military, *Environ. Sci. Technol.* 46 (2012) 7120–7127.
- [6] C.A. Moody, J.A. Field, Perfluorinated surfactants and the environmental implications of their use in fire-fighting foams, *Environ. Sci. Technol.* 34 (2000) 3864–3870.
- [7] K. Shinoda, T. Nomura, Miscibility of fluorocarbon and hydrocarbon surfactants in micelles and liquid mixtures. Basic studies of oil repellent and fire extinguishing agents, *J. Phys. Chem.* 84 (1980) 365–369.
- [8] J. Scheffey, R. Darwin, J. Leonard, Evaluating firefighting foams for aviation fire protection, *Fire Technol.* 31 (1995) 224–243.
- [9] L.A. D'Agostino, S.A. Mabury, Identification of novel fluorinated surfactants in aqueous film forming foams and commercial surfactant concentrates, *Environ. Sci. Technol.* 48 (2013) 121–129.
- [10] C.A. Moody, J.A. Field, Determination of perfluorocarboxylates in groundwater impacted by fire-fighting activity, *Environ. Sci. Technol.* 33 (1999) 2800–2806.
- [11] L. Ahrens, K. Norström, T. Viktor, A.P. Cousins, S. Josefsson, Stockholm Arlanda Airport as a source of per- and polyfluoroalkyl substances to water sediment and fish, *Chemosphere* (2014) (in press).
- [12] E.F. Houtz, C.P. Higgins, J.A. Field, D.L. Sedlak, Persistence of perfluoroalkyl acid precursors in AFFF-impacted groundwater and soil, *Environ. Sci. Technol.* 47 (2013) 8187–8195.
- [13] M.E. McGuire, C. Schaefer, T. Richards, W.J. Backe, J.A. Field, E. Houtz, D.L. Sedlak, J.L. Guelfo, A. Wunsch, C.P. Higgins, Evidence of remediation-induced alteration of subsurface poly- and perfluoroalkyl substance distribution at a former firefighter training area, *Environ. Sci. Technol.* 48 (2014) 6644–6652.
- [14] N. Ratola, A. Cincinelli, A. Alves, A. Katsoyiannis, Occurrence of organic microcontaminants in the wastewater treatment process. A mini review, *J. Hazard. Mater.* 239–240 (2012) 1–18.
- [15] O. Weiß, G.A. Wiesmüller, A. Bunte, T. Göen, C.K. Schmidt, M. Wilhelm, J. Hölzer, Perfluorinated compounds in the vicinity of a fire training area – human biomonitoring among 10 persons drinking water from contaminated private wells in Cologne, Germany, *Int. J. Hyg. Environ. Health* 215 (2012) 212–215.
- [16] S.R. de Solla, A.O. De Silva, R.J. Letcher, Highly elevated levels of perfluorooctane sulfonate and other perfluorinated acids found in biota and surface water downstream of an international airport, Hamilton, Ontario, Canada, *Environ. Int.* 39 (2012) 19–26.
- [17] E. Awad, X. Zhang, S.P. Bhavsar, S. Petro, P.W. Crozier, E.J. Reiner, R. Fletcher, S.A. Tittlemier, E. Braekevelt, Long-term environmental fate of perfluorinated compounds after accidental release at Toronto airport, *Environ. Sci. Technol.* 45 (2011) 8081–8089.
- [18] K.D. Oakes, J.P. Benskin, J.W. Martin, J.S. Ings, J.Y. Heinrichs, D.G. Dixon, M.R. Servos, Biomonitoring of perfluorochemicals and toxicity to the downstream fish community of Etobicoke Creek following deployment of aqueous film-forming foam, *Aquat. Toxicol.* 98 (2010) 120–129.
- [19] L.W.Y. Yeung, S.A. Mabury, Bioconcentration of aqueous film-forming foam (AFFF) in Juvenile rainbow trout (*Oncorhynchus mykiss*), *Environ. Sci. Technol.* 47 (2013) 12505–12513.
- [20] S.B. Gewurtz, S.P. Bhavsar, S. Petro, C.G. Mahon, X. Zhao, D. Morse, E.J. Reiner, S.A. Tittlemier, E. Braekevelt, K. Drouillard, High levels of perfluoroalkyl acids in sport fish species downstream of a firefighting training facility at Hamilton International Airport, Ontario, Canada, *Environ. Int.* 67 (2014) 1–11.
- [21] R. Dorf, *Engineering Handbook*, CRC Press, New York, 1996.
- [22] J.L. Guelfo, C.P. Higgins, Subsurface transport potential of perfluoroalkyl acids at aqueous film-forming foam (AFFF)-impacted sites, *Environ. Sci. Technol.* 47 (2013) 4164–4171.
- [23] K.-U. Goss, The pK<sub>a</sub> values of PFOA and other highly fluorinated carboxylic acids, *Environ. Sci. Technol.* 42 (2007) 456–458.
- [24] D. Brooke, A. Footitt, T. Nwaogu, G. Britain, Environmental Risk Evaluation Report: Perfluorooctanesulphonate (PFOS), Environment Agency Wallingford, 2004.
- [25] J.W. Washington, H. Yoo, J.J. Ellington, T.M. Jenkins, E.L. Libelo, Concentrations, distribution, and persistence of perfluoroalkylates in sludge-applied soils near Decatur Alabama, USA, *Environ. Sci. Technol.* 44 (2010) 8390–8396.
- [26] J. Chorover, M.L. Brusseau, Kinetics of sorption–desorption, in: S.L. Brantley, J.D. Kubicki, A.F. White (Eds.), *Kinetics of Water–Rock Interaction*, Springer, New York, 2008, pp. 109–149.
- [27] J.G. Sepulvado, A.C. Blaine, L.S. Hundal, C.P. Higgins, Occurrence and fate of perfluorochemicals in soil following the land application of municipal biosolids, *Environ. Sci. Technol.* 45 (2011) 8106–8112.
- [28] J. Thompson, G. Eaglesham, J. Reungoat, Y. Poussade, M. Bartkow, M. Lawrence, J.F. Mueller, Removal of PFOS, PFOA and other perfluoroalkyl acids at water reclamation plants in South East Queensland Australia, *Chemosphere* 82 (2011) 9–17.
- [29] C. Baduel, F.Y. Lai, K. Townsend, J.F. Mueller, Size and age–concentration relationships for perfluoroalkyl substances in stingray livers from eastern Australia, *Sci. Total Environ.* 496 (2014) 523–530.

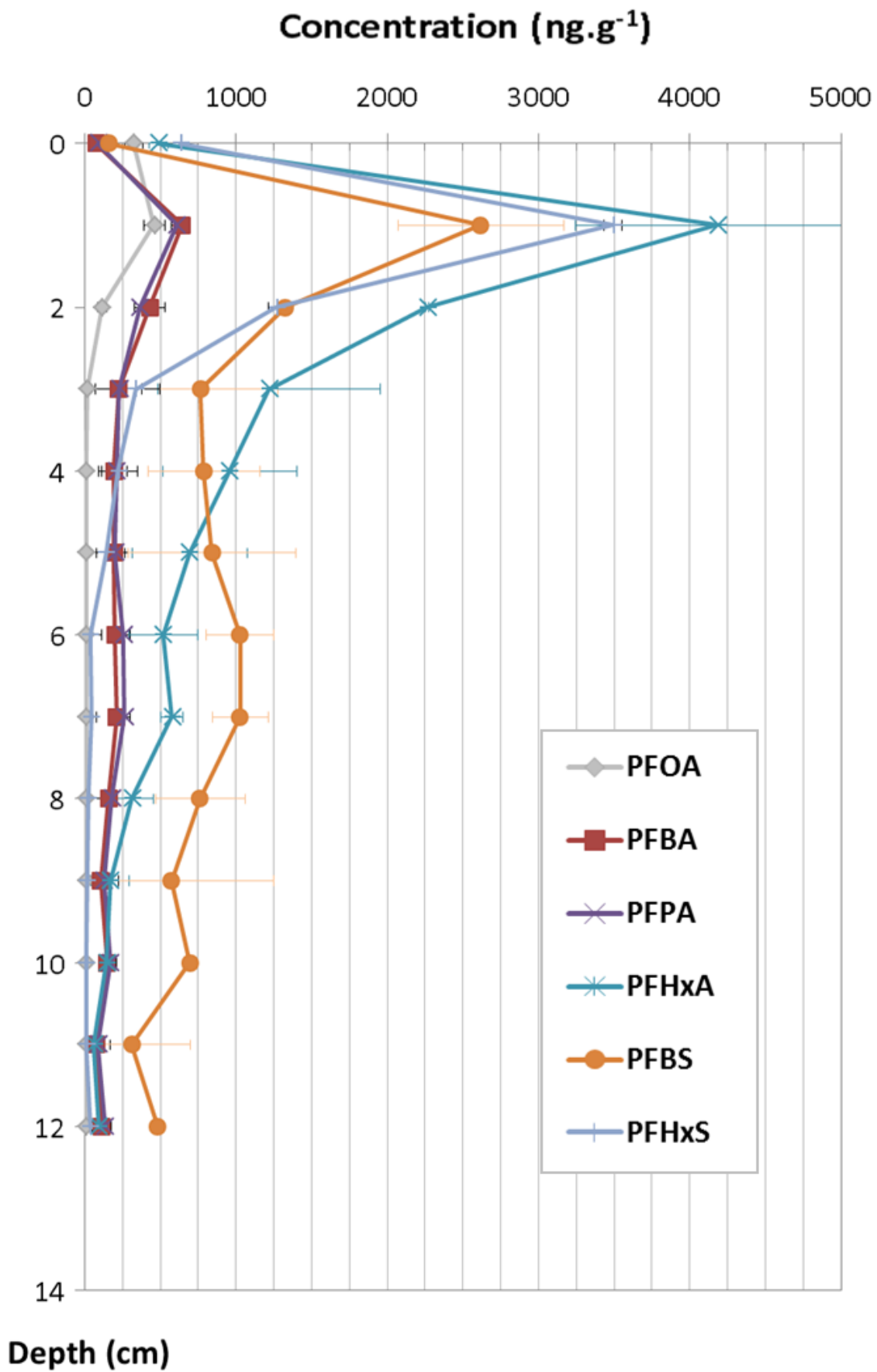


	PFBA		PFPA		PFHxA		PFHA		PFOA		PFNA		PFDeA		PFUnA		PFDoA		PFTriA		PFTeA	
	Profile 1	Profile 2	Profile 1	Profile 2	Profile 1	Profile 2	Profile 1	Profile 2	Profile 1	Profile 2	Profile 1	Profile 2	Profile 1	Profile 2	Profile 1	Profile 2	Profile 1	Profile 2	Profile 1	Profile 2	Profile 1	Profile 2
0 ± 0.2	69	80	82	98	443	534	78	97	280	365	339	579	3,621	3,107	2,275	2,422	1,675	1,814	300	298	376	370
0.8 - 1.2 cm	661	627	569	652	3,520	4,851	461	672	408	507	<6	<6	<12	<12	<3	4	<10	<10	<3	<3	<5	<5
1.8 - 2.2 cm	503	359	407	326	2,274	2,260	238	234	137	91	<6	<6	<12	<12	<3	4	<10	<10	<3	<3	<5	<5
2.8 - 3.2 cm	333	117	339	116	1,739	698	72	31	21	<10	<6	<6	<12	<12	6	<3	<10	<10	<3	<3	<5	<5
3.8 - 4.2 cm	255	135	302	121	1,272	645	35	13	8	<10	<6	<6	<12	<12	<3	5	<10	<10	<3	<3	<5	<5
4.8 - 5.2 cm	278	113	287	113	961	425	17	11	6	<10	<6	<6	<12	<12	<3	4	<10	<10	<3	<3	<5	<5
5.8 - 6.2 cm	204	196	310	207	360	680	<2	7	<10	<10	<6	<6	<12	<12	<3	<3	<10	<10	<3	<3	<5	<5
6.8 - 7.2 cm	201	225	287	240	629	524	5	4	<10	<10	<6	<6	<12	<12	6	4	<10	<10	<3	<3	<5	<5
7.8 - 8.2 cm	177	144	238	125	414	215	4	<2	<10	<10	<6	<6	<12	<12	5	<3	<10	<10	<3	<3	<5	<5
8.8 - 9.2 cm	25	190	25	233	79	257	2	<2	<10	<10	<6	<6	<12	<12	3	<3	<10	<10	<3	<3	<5	<5
9.8 - 10.2 cm	136	160	152	186	144	146	<2	<2	<10	<10	<6	<6	<12	<12	<3	3	<10	<10	<3	<3	<5	<5
10.8 - 11.2 cm	14	139	11	165	11	112	<2	3	<10	<10	<6	<6	<12	<12	<3	4	<10	<10	<3	<3	<5	<5
11.8 - 12.2 cm	120	109	142	127	108	76	7	5	<10	<10	<6	<6	<12	14	12	7	<10	<10	<3	<3	<5	<5

	PFBS		PFHxS		PFOS		PFDS		62FTS 1	
	Profile 1	Profile 2	Profile 1	Profile 2	Profile 1	Profile 2	Profile 1	Profile 2	Profile 1	Profile 2
0 ± 0.2	164	153	540	729	217,587	237,409	416	531	17	26
0.8 - 1.2 cm	2,231	3,007	3,163	3,825	4,427	4,893	<10	<10	458	<13
1.8 - 2.2 cm	1,328	1,325	1,452	1,088	1,937	1,147	<10	<10	242	<13
2.8 - 3.2 cm	1,130	401	503	168	558	120	<10	<10	152	<13
3.8 - 4.2 cm	1,050	527	346	96	249	64	<10	<10	63	<13
4.8 - 5.2 cm	1,235	451	226	59	167	195	<10	<10	43	<13
5.8 - 6.2 cm	1,186	868	10	64	41	238	<10	<10	<13	<13
6.8 - 7.2 cm	1,159	900	58	29	228	131	<10	<10	20	<13
7.8 - 8.2 cm	971	554	36	14	258	57	<10	<10	15	<13
8.8 - 9.2 cm	93	1,054	24	9	151	42	<10	<10	<13	<13
9.8 - 10.2 cm	721	670	10	9	51	37	<10	<10	<13	<13
10.8 - 11.2 cm	39	586	<5	17	44	95	<10	<10	<13	<13
11.8 - 12.2 cm	504	461	33	43	725	997	<10	<10	<13	<13

Concentration interval (ng g<sup>-1</sup>)





Sampling position	Concentration (ng g <sup>-1</sup> )																Σ PFASs
	PFBA	PFPA	PFHxA	PFHA	PFOA	PFNA	PFDeA	PFBS	PFHxS	PFOS	PFUnA	PFDoA	PFTriA	PFTeA	PFDS	62FTS 1	
Blank	< 5	< 6	< 1	< 2	< 5	< 6	< 12	< 5	< 5	< 3	< 3	< 10	< 3	< 5	< 10	< 13	
1	97	19	63	58	76	< 6	< 12	30	220	345	8	49	57	60	< 10	29	1,111
2	94	64	276	55	143	25	32	57	452	3,115	85	323	260	257	20	46	5,305
3	31	21	105	62	104	15	37	16	118	700	31	480	453	450	15	37	2,676
4	36	29	168	91	623	83	30	54	1,548	2,657	18	56	32	33	< 10	553	6,010
5	44	28	151	66	182	11	< 12	30	305	1,385	28	153	114	85	< 10	86	2,669
6	48	24	88	38	110	13	< 12	37	186	635	21	152	254	238	< 10	33	1,877
7	145	206	1,314	434	930	32	63	372	2,015	39,048	60	102	32	32	25	156	44,966
8	52	23	101	46	113	22	41	24	115	633	124	794	352	279	20	23	2,762
8-duplicate	60	29	134	80	185	25	44	24	148	756	134	963	402	329	30	68	3,413
9	373	426	2,601	488	917	70	169	1,751	4,391	22,870	424	646	240	105	163	95	35,729
10	161	174	1,061	417	1,259	180	2,413	266	2,029	101,125	1,885	1,768	253	310	316	302	113,919
11	659	530	3,749	612	618	25	72	2,177	2,450	3,415	148	603	266	245	10	39	15,619
12	264	295	1,407	283	598	207	6,641	1,912	2,734	203,857	3,880	1,848	481	624	297	29	225,358
13	25	16	83	31	135	21	68	11	146	960	878	2,698	594	538	35	28	6,267
14	149	211	1,006	191	651	1,009	5,614	746	1,491	223,983	4,505	2,626	564	1,017	473	57	244,294
15	23	14	87	232	89	< 6	< 12	34	228	79	6	26	15	20	< 10	25	877

Concentration interval (ng g <sup>-1</sup> )	
C < LOQ	Lower than LOQ
LOQ < C < 100	Concentration between LOQ and 100 ng g <sup>-1</sup>
100 < C < 1000	Concentration between 100-1,000 ng g <sup>-1</sup>
1,000 < C < 10,000	Concentration between 1,000-10,000 ng g <sup>-1</sup>
10,000 < C < 100,000	Concentration between 10,000-100,000 ng g <sup>-1</sup>
100,000 < C < 1,000,000	Concentration superior at 100,000 ng g <sup>-1</sup>